*Original article*

# DOCUMENTING OIL PAINTINGS BY FINGERPRINT BRUSHSTROKE APPLICATION TO ANTIQUE PAINTING IN THE EGYPTIAN MUSEUM OF MODERN ART

Abo-Taleb Th.

*Conservation dept., Faculty of Archaeology, Aswan Univ, Aswan, Egypt*
*E-mail*: sanna_abotaleb@yahoo.com

## Abstract

*The present study discusses documenting a topographic surface in an oil painting by remote sensing. It is a new technological method in documenting the properties of the brush texture statistically, including the area, width, length, the shape of ends of the edges lines of the hair (curve, point, or polygon), directions, as well as the angle among these edges and surfaces. Then, the study carries out a quantitative evaluation of signature spectral fingerprint of the brush areas. It examines the spatial distribution of the texture and the spectral recording of the color by recording the reflected or emitted radiation from the colors varying in absorption, penetration, and reflection according to the physical and chemical properties of each substance, forming the so-called signature spectral fingerprint. Using the ENVI sensor program to check the texture of the brush in the visual part and find statistical patterns which helps us to identify the optical properties of the brush strokes and artist style. The result of the texture analysis revealed that the brush was flat, with hard hair, parallel lines, and perpendicular angles. The spectral signature of orange was (591.08 nm), pink was (495.87 nm) (595.2 nm), adobe was (600.93 nm), and dark brown was (579.55 nm). The brushstroke's area equaled 49248, and the perimeter measured 888. Furthermore, SEM-EDX, XRD, and FTIR were utilized to define the materials and methods of three colored samples of oil painting (red, yellow, and green). Results illustrated that the samples contained linseed oil as binders and ground layer from calcite mixed with animal glue. SEM-EDX and XRD results pointed out that the pigment samples were earth pigments (goethite - Hematite - Celadonite).*

## 1. Introduction

Remote sensing is one of the most useful sciences for extracting useful information related to the propagation of the electromagnetic waves across the surface, quality, and condition of the target. The energy is sent by the target depending on the wavelength. For each material, which mainly depends on its surface characteristics, this technology has helped to explain ancient papyri, such as those found in Herculaneum, by imaging the parts in the infrared (1000 nm) range. The text in the documents often appears to the naked eye as black ink on black paper. In the 1000 nm range, the difference reflected by light makes the text clearly readable. It was also used to depict Archimedes' "compositions by depicting manuscript papers in a bandwidth of 365-870 nm and then using modern digital image processing methods to show the embedded text of Archimedes" works [1]. Later, digital data processing helped to create data and images for different applications and tasks

without having a direct physical contact with the information capture device to obtain images, special information, reflectance data, and spectral behavior of things. These numerical values were analyzed on a computer using special software, such as ENVI 5, to obtain results in the form of graphs, maps, images, tables, and statistical reports. Remote sensing cameras use the energy of visible light because some painters utilize different technical methods in applying colors on the surface of the painting, including painting with various thickness texture resulting from the density of colors in which the brushstroke appear. The brushstroke depends on transforming the resulting lines into geometric shapes and extracting the shape of the edges into the curve, point, or polygon using software; it collects, analyzes, displays, and extracts descriptive information from its position and shape (the brush edges). It also displays the length, depth, and area of the brushstroke. Then, the results of the surface of the painting are inserted in a table. The stages are arranged according to using ENVI 5 transform oil painting to the digital image, dividing it into parts or elements. In appropriate operating conditions of light and camera are vertically positioned on the painting [2]. The painting is represented in two ways: The first way is bounded to the external form of the brush or a surface presentation; while the second one is a survey of the inner features and defines shapes through a process that handles every pixel in the painting using a filter [3] to outline the edges. The brush is reinforced to achieve a better view for improving the details [4] of the brush texture. This process is achieved by enlarging the brush [5] and transforming it into geometric shapes that define its edges [6] in the space of colors, fig. (1-a,b). The pixel has been widely used to represent information on color [7], texture, brightness, color gradations, and defining edges [8]. The mask is applied to each pixel to form the edge [9] and identify the trend of the brush in all pixels [10] using ENVI

5 software. ENVI 5 studies the texture of the brush by defining all points where the endings of the bristles appear. The wavelength of the points of the components of each pixel is calculated. Each pixel has a digital value in this area ranging from 0 to 255 representing the amount of radiation specified by ENVI 5 [11]. The color of digital image can be represented using three main colors, i.e. red, green, and blue (RGB) [12], Specifying the values of color intensity for each pixel, define the geometric shape and dimensions of the brush aims to show the edges of the external line and the direction of the brush [13] using a filter that marks the edges, then calculating the color value [14] in the brushstroke through the number of pixels' color. Images differ in the number of colors according to the number of bits in each pixel [15]. The points of the brushstroke's position are identified in the painting to get its location a measurement of area [16]. Thus, a table of the coordinates should be created and data should be sorted and saved in the form of a matrix. When the computer tests the brushstroke, it compares numbers of their color components [17] in the memory of the computer with the inserted one [18]. the value of the color component represents the physical properties of the brushstroke [19] In addition, a multispectral image is obtained in a small range of visible spectra, ranging from 0.4 to 0.7 nm, called red-green-blue (RGB), switching to infrared waves from 0.7 to 1 nm or more and classified as Near Infrared (NIR), Medium Infrared (MIR) and Far (or Thermal) Infrared. It uses real color channels of red, green, and blue only assigned to their respective colors. [20]. The oil painting under study dating back to the late 18th century was carried out on the canvas. It was kept in the store of the Museum of Modern Art, Cairo Opera House, Ministry of Culture. It is in the Inventory's logbook number 79 and measures (45 x 60 cm). It has a strong technical style showing a landscape of a group of houses on brown background accurately and beautifully; fig. (1-c,d).
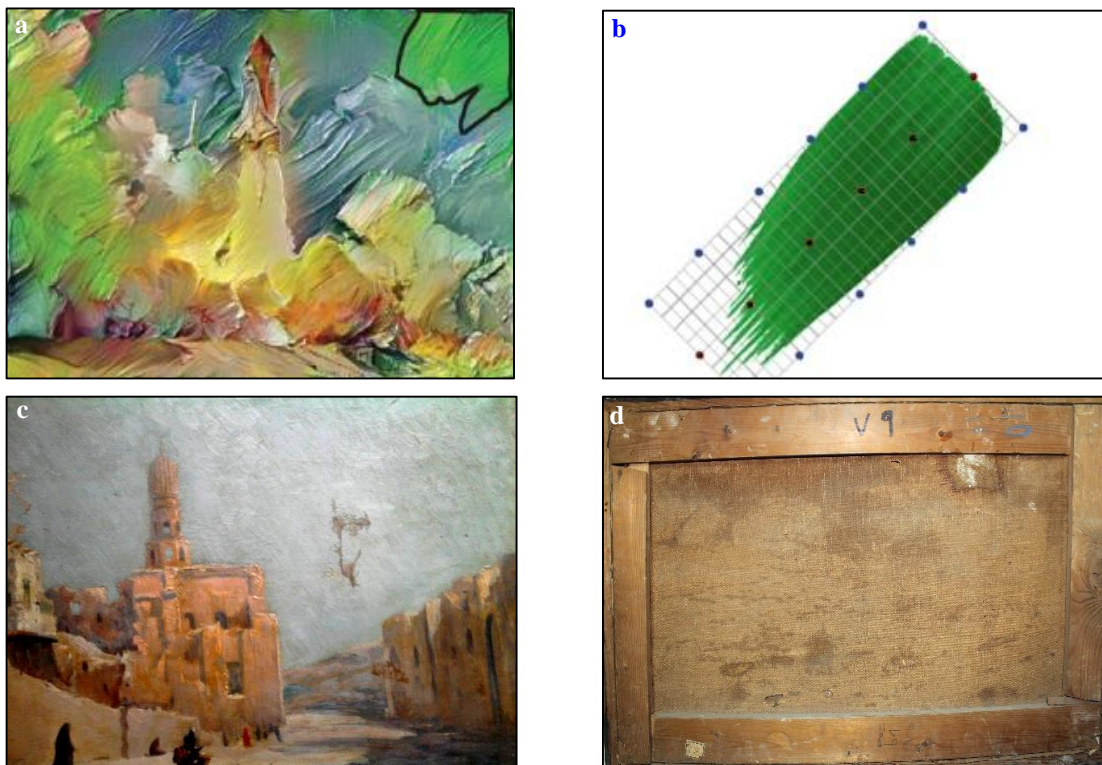
Figure (1) Shows **a.** & **b.** the stages extraction brush line and shape, **c.** the front of archaeological painting in, **d.** the back of archaeological painting

## 2. Materials and Methods
### 2.1. *Materials*

The study was conducted on three samples from colors yellow, green, and red. All samples contained the ground layer. Various examinations and analyses were perfo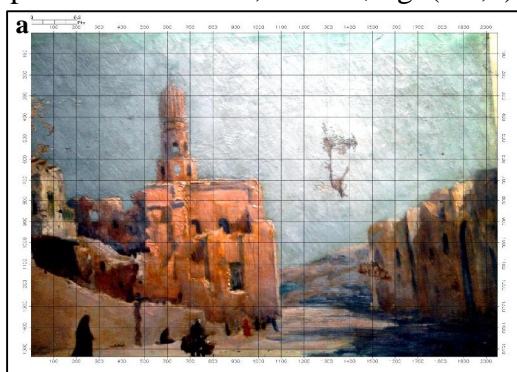rmed using different techniques to study the painting's materials. Complementary analysis of the brush texture was done by extracting the physical properties of the brush including appearance (e.g. brightness/color gradient) and texture.

### 2.2. *Methods*

Various methods of examination and analysis were utilized to investigate and interpret the degradation manifestations of the painting. Visual examination (visible light) is used in the first stage of the examined painting. Such examination is often aided by the magnifiers glasses (4:6-x) to zoom in a brushstroke. The direction in which the light falls on the painting can show the technical features and the deterioration of the painting, e.g. cracks. The direction in which the light source is located to one side of the object at a low angle between 5º and 30º [21] emphasizes the painting layer texture's brushstrokes. It shows the artist's technicalities, e.g. impastos, and the different aspects of deterioration, such as flaking paint. It also indicates the areas that require conservation attention. The results of the visible light examination are recorded with standard photography techniques [22]. Examination was done using optical microscopy (OM) with a Nikon digital 56 camera DMX 1200 F, a mercury lamp, and a halogen lamp, allowing conservators to study techniques of artist [23]. Digital microscope was used to check some areas of the brushstroke [24] and identify the painter's techniques [25]. SEM was employed for providing detailed information on the degradation of the surface painting [26], while EDX was used for the qualitative analysis of the elements' ratios presented in the pigments. This helped reveal the structure of the colored layer [27] The operating system the electron beam's high voltage was 20 KeV, and the magn-

nification varied (500x-1000x) with a resolution of 3.5 nm and X-Ray mapping yielding distribution of the element in the different paint layers [28]. XRD was used for the crystallography structural analysis and of the object, which is a characteristic of the artist [29]. In addition, FTIR analysis was done for determining the inorganic compounds. The chemical composition of the active collections of historical samples was determined and compared with the standard samples. Therefore, their operating conditions conform to the same operating conditions of the archaeological samples (Resolution=4 cm-1; Scans120; Range=

4000-400 cm-1) [30]. The resulting absorption spectrum is a characteristic of each compound. By defining this wavelength and the absorption areas, the compound is identified through its active groups compared with standard samples [31]. Finally, texture brushstroke's extraction through the edge of contour was analyzed using an ENVI 5 image. Spectral imaging giving information about the texture of the brush related to its various absorption properties of different light wavelengths was obtained.

### 2.2.1. Analysis of the brushstroke using ENVI 5 (*Remote Sensing*)

To be similar to the digital image to the original painting, put a camera vertically fixed on a stand at 112 cm with 45°C [32] to avoid the reflection; the lighting is like daylight consisting of four fluo-rescent bulbs type Aux Dulux L36W/954k. The image captures the highest resolution. It is saved and stored in an uncompressed format, such as the 16-bit TIFF format. Then, open the image in senior ENVI 5 [33]. The digital image consists of some small squares stacked next to each other and it is an array of columns (c) and rows (r). Each square represents an element or a unit of the image (pixel). These small units spatially represent areas. They are a small ground for preparing digital image data for statistical studies. The oil painting under study was drawn by a 1: 5 scale and divided into pixels, where each pixel has an integer value from 0 to 255. The image is divided based on a density number of the color of the gradient in the panel, fig. (2-a,b). Then, the texture brush position is selected, zoomed, fig. (2-c,d);

and converted to lines by the direction [34] of the brushstroke area defined by extracting its external edges. Color is measured and usually rep-resented by three components representing its three-dimensional coordinates in the color space that simulates the human eye to measure it with a numerical value. ENVI 5 is utilized to show the boundary of the brush texture, size, and area. The result was the percentages of the value of color use in texture and movement of all pixels [35] in brush scaled by specifying co-ordinates (X and Y) values for each point's geometric form quadrilateral or polygonal shape. Then, the mask was applied to get the brushstroke properties such as color tone [36], length, width, and angle among the external edges (shape, size) [37]. It illustrated the wavelengths of blue, green, and red in the brushstroke. Spectral refle-ctions were recorded in spectral beams ranging from (350 nm) to (2500 nm) near the infrared spectrum and the visible infrared spectrum (MIR).
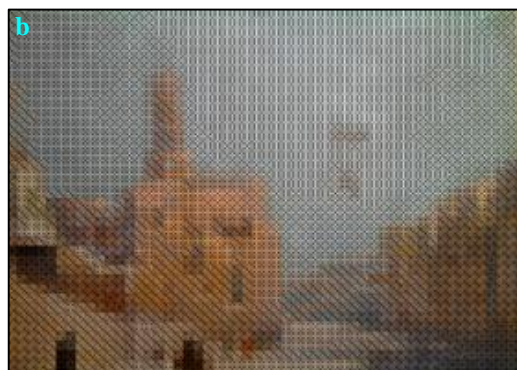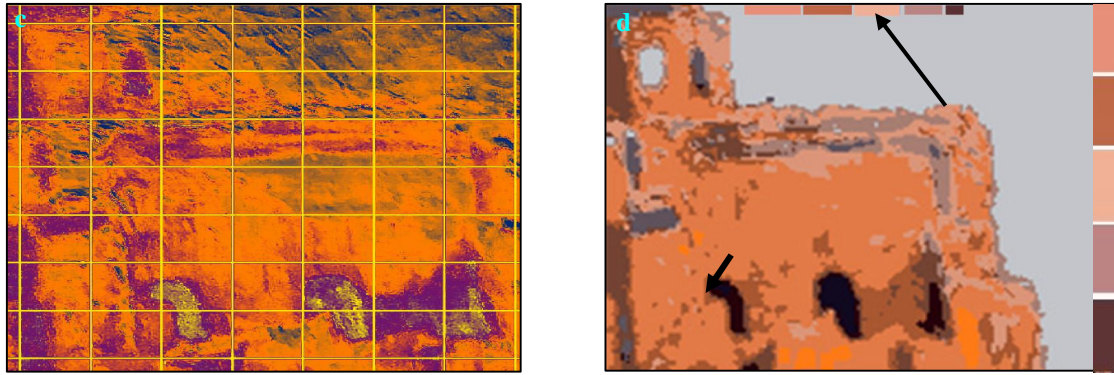
Figure (2) Shows **a.** drawingby (1:5) scale, **b.** dividing the image based on optical density, **c.** zoom texture of the brush, **d.** tone colored in area of brush

## 3. Results
### 3.1. *Visual and reflected light examination*

Electronic flash lamps showed both structural and aesthetic problems, primarily due to water exposure. The varnish was very yellow, and the dirt and dust were on the painting's surface and inside the cracks.

### 3.2. *Light and digital microscopes*

The examination of a yellow sample magnification (20-x), fig. (3-a) illustrated the painter's technical style. The layered structure of painting on the fabric was four layers: support layer, gesso layer, and two paint layers [38]. The painter applied a yellow wet pigment layer on a red dry layer in the house [39]; and the digital microscope showed the style of color application by scratching through a layer of still-wet paint to reveal what's underneath. This technique is called sgraffito, a form of decoration made by scratching using a hard brush through a surface to reveal a lower layer of a contrasting color. It uses roughly parallel and/ or crossed strokes to indicate shading the brushstrokes achieving angled strokes [40]. It is mainly done for stylistic purposes in using color in texture in the sky and the house. The results pointed out that the texture of the brush direction was parallel to the house, fig. (3-b).
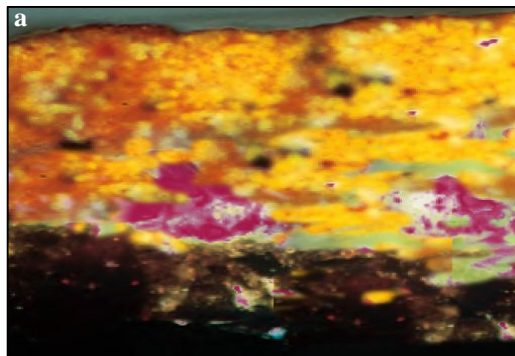


Figure (3) Shows **a.** OM of a cross-section sample color yellow, (20x), **b.** sgraffito technique in some areas in house

### 3.3. *EDX-SEM analysis*

The analysis results of the three pigments with SEM and EDX are listed in tab. (1) & fig. (4-a,b,c). SEM results showing the surface's degradation, cracks, pits, and deposition layer, as well as colored elements mapping of detail pointed element coexistence in all samples (Fe, Mg, Al, Si, Ca, O, C, Na, and K). Furthermore, clay was in all samples (Ba, Ti, and S) were found in the green map and (S and Pb) were found in yellow map, fig. (4-d,e,f).

Table (1) Elemental ratios (%) results by EDX analysis of the various painting samples

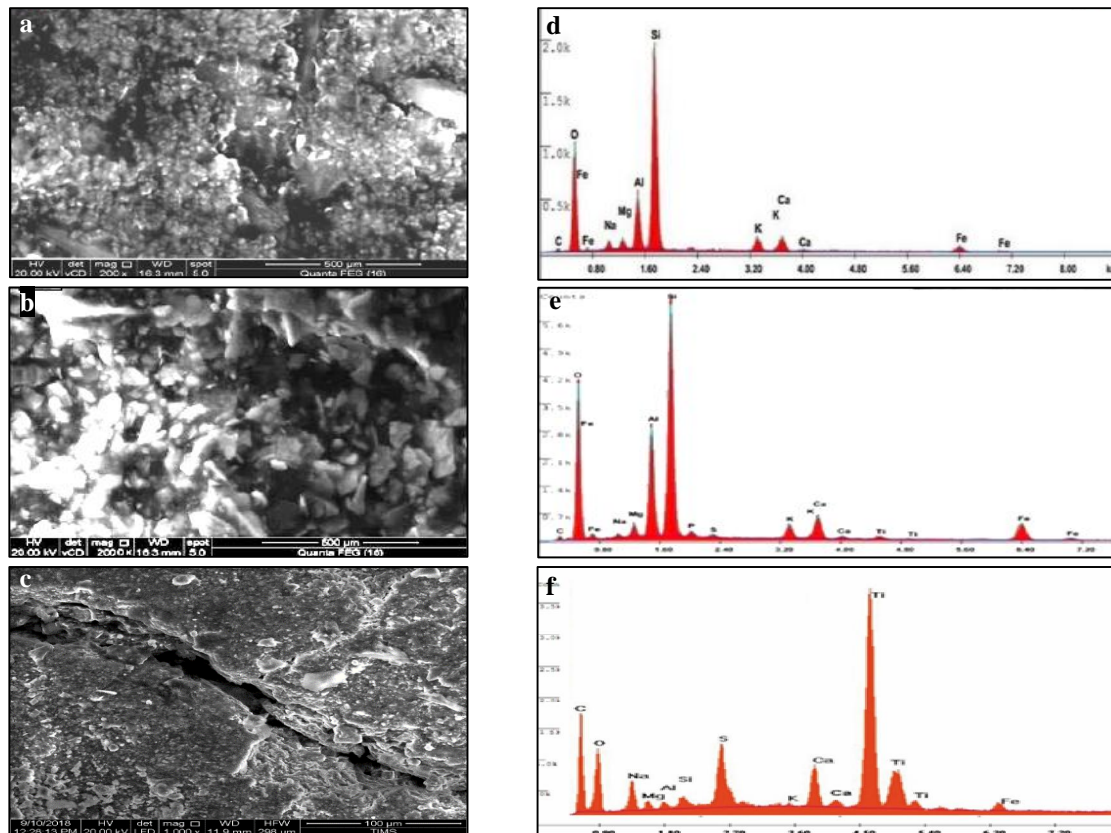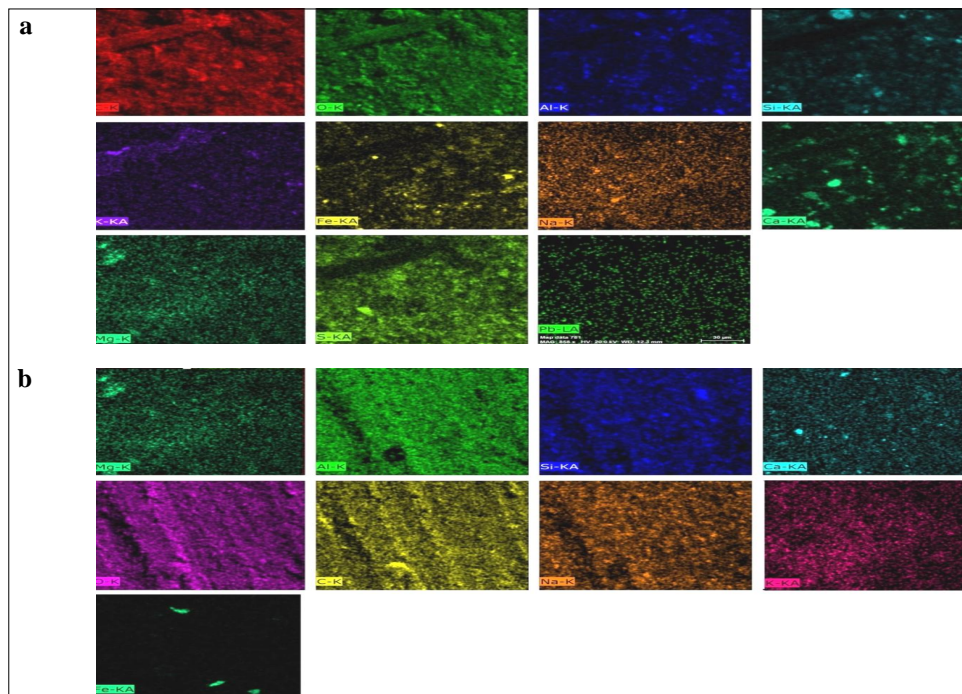| Samples | C | O | Na | Mg | Al | Si | K | Ca | Fe | S | Pb | Ba | Ti |
|---------|------|------|-----|-----|------|------|-----|-----|------|-----|-----|-----|------|
| **Red** | 3.3 | 32.0 | 1.6 | 1.6 | 8.7 | 36.0 | 4.4 | 5.0 | 7.6 | - | - | - | - |
| **Yellow** | 2.5 | 29.7 | 0.5 | 1.4 | 12.1 | 26.2 | 3.0 | 5.3 | 14.7 | 0.4 | 2.9 | - | - |
| **Green** | 33.5 | 17.1 | 2.1 | 0.7 | 0.5 | 1.4 | 5.1 | 0.9 | 8.2 | 2.4 | - | 4.0 | 25.2 |



Figure (4) Shows SEM of **a.** Red sample (200x), **b.** yellow sample (2000x), **c.** green (1000x), **d., e. & f.** EDX charts of the same samples
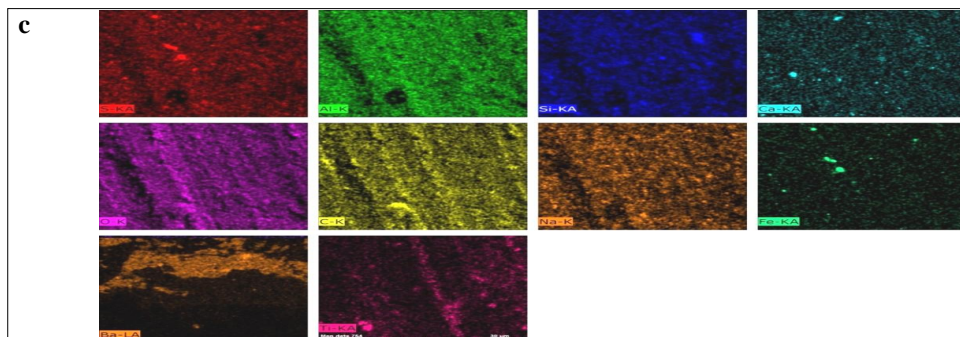
Figure (4) Shows elemental colored mapping of detail distribution of ca, Al, si, Na, k, Fe (*the main components of clay*) **a.** red sample, **b.** yellow sample, **c.** green sample

## 3.4. *X-ray diffraction analysis (XRD)*

XRD results revealed that all painting samples were earth pigments. They may be broadly divided into iron-rich ochres (iron oxide and oxide hydroxide). The earth pigments are not pure, the property of being mixtures of possibly several minerals like clays, carbonates and quartz. The results, fig. (5-a,b) illustrated that yellow and red contained gypsum. $CaSO_4.2H_2O$ appeared in card no. (04-008-9805) as a major component (79.6%) as a result of bad storage and exposure to moisture that turned the calcite in the ground layer into calcium sulphate.

The red sample $Fe_2O_3$ appeared in card no. (01-080-5407) (14.5%). NaCl appeared in card no. (01-076-3454) (0.6%). The yellow color sample pointed out that calcite ($CaCO_3$) card no. (01-081-9559) as a main component rating (73.2%) resulted from the ground layer. These results matched SEM and FTIR analyses and showed FeO (OH) card no. (04-015-8212) (13.9%) and $Fe_2O_3$ card No. (01-088-2359) (12.9%). Their presence pointed out that they are compounds of yellow earth pigment.
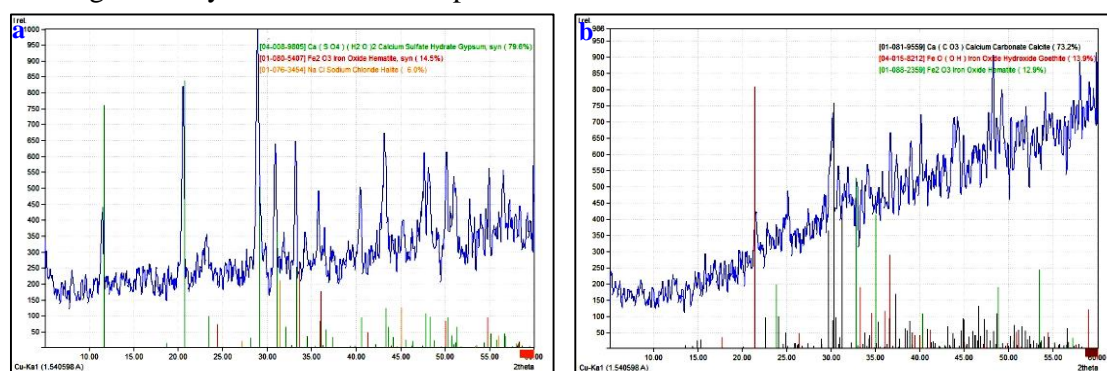


Figure (5) Shows XRD patterns of **a.** red sample, **b.** yellow sample.

## 3.5. *Fourier transform infrared (FTIR)*

The results of FTIR, fig. (6-a) illustrated that the adhesive used in the ground layer was rabbit glue mixed with calcite. The appearance of the wavelength at (1633.774 cm$^{-1}$) indicated (amide I) and the wavelength at (1593.257 cm$^{-1}$) indicated (Amide II (N–H) bending) mixed with calcite which was clearly identified by the absorption band wavelength at (1455.894 cm$^{-1}$) indicating (CO-stretching band) [41]. In addition, fig. (6-b) pointed out that the color mixed with linseed oil at the absorption bands wavelength (3381.084 cm$^{-1}$) suggested OH, which is generally assigned to the stretching of alcohol and hydro peroxide bonds formed because of the polymerization and aging in the oil film during which the double bonds present in the triglyceride moieties underwent oxidation [42]. While the absorption band wavelength at (2925.082 cm$^{-1}$) indicated ($CH_2$), the absorption band wavelength at (1733. 774 cm$^{-1}$) indicated (C=O) [43], the absor-

147

ption band wavelength at (1455.894 cm$^{-1}$) suggested (C–H bending), and the absorption band wavelength at (971.541 cm$^{-1}$) indicated (C-O stretching bands) [44].

This result suggested the existence of vegetable oils linseed oil as a color medium. The FTIR spectrum of the binding media was similar to the ones made of linseed oil.
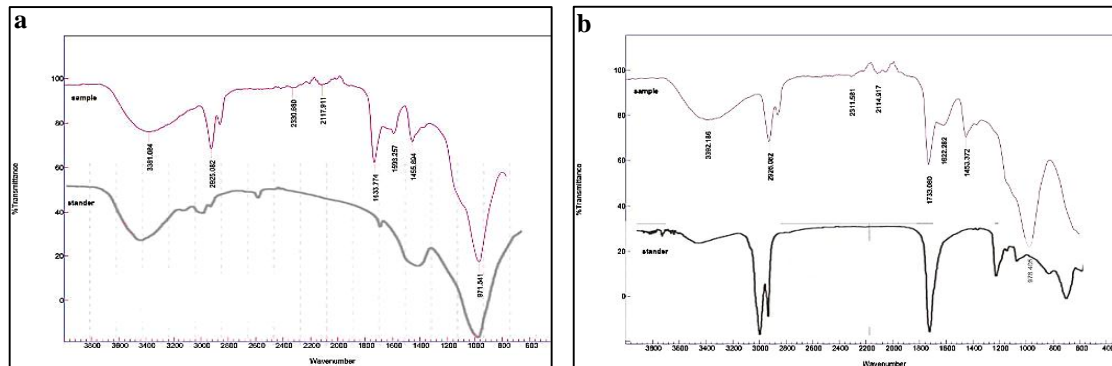


Figure (6) Shows **a.** the unknown and standard calcite mixing with animal glue samples, **b.** the unknown and standard calcite mixing with linseed oil
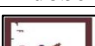
## 3.6. *Texture analysis*

Conducting a statistical survey of each colored area in the brushstroke, each cell pixel represents a color area, assigning it a numerical value. Table (2) and fig. (7-a) show percentages of all color tones values [45] and code colored model for color theory. They describe the perceptions of the color component based on the percentages of the red, blue, and green values in the color tone and value angle (hue) between the statistical distance color scales [46]. Furthermore, the values, tone, lightness, saturation, and wavelengths of red, blue and green [47] allow us to study the colors scientifically using ENVI 5. The analysis pointed out that the tones in the area texture brush were the light orange code (#de7e4a), 87.06% of the component was red, 49.41% was green, and 29.02% was blue. For the HSL, the color space had a hue of 21°, saturation 69%, lightness of 58%, and a wavelength of 591.08 nm. For the sweet pink tone code (#faccd6), 98.04% of the component was red, 80% was green, and 83.92% was blue. In the HSL, the color space had a hue of 347°, saturation of 82%, lightness of 89%, and a wavelength of 495.87 nm. In the orchid pink tone color code (#e5bdb5), 89.8% of the component was red, 74.12% was green, and 70.98% was blue. In the HSL, the color space had a hue of 10°, saturation of 48%, lightness 80%, and a wavelength of 595.2 nm. For the adobe tone code (#4e402c), 30.59% of the component was red, 25.1% was gre-en, and 17.25% was blue. In the HSL, the color space had a hue of 35°, saturation of 28%, lightness of 24%, and a wavelength of 579.55 nm. For the brown drake tone code (#580000), 34.51% of the component was red, 25.01%% was green and 17.25% was blue. In the HSL, the color space had a hue of 25°, saturation of 28%, lightness of 17%, and a wavelength of 611.37 nm. Then, the external line of the brush was obtained. Furthermore, fig. (7-a) showed the brush [48] by ENVI5. The value of (x, y) was calc-ulated from one end of the outer limits of the brush lines in (x=170, y= 295). The total area of the brushstroke's pixels equaled 50150 pixels, while the perimeter equaled 888. The program gave spectral information about the electro-magnetic spectrum for each element (pixel) in the brushstroke. It also gave (spectral scanning) at different wavelengths in the visible, short and long wave infrared regions of the electromagnetic spectrum. It is more important for the brushstroke discrimination to use this technique bec-ause it depends on the amount of radiation from the brush area and the roughness and softness of the surface. Each area of the colored tone appeared distinctively from the rest of the material called the [spectral signature [49] that equalled (0.045/0.51 µm), (0.53/0.59 µm), and (0.64/0.67µm) for the wavelengths of blue, green, and red respectively, fig. (7-b).

Table (2) The percentages of the colors' tone, hue angle, and wavelength in the brushstroke

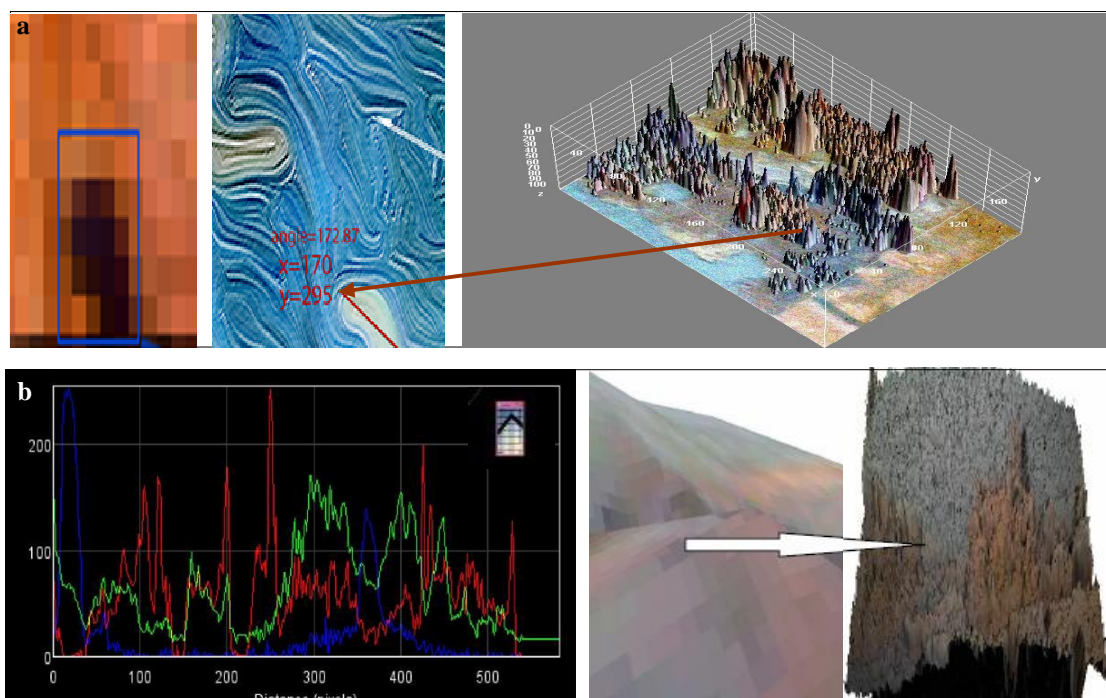| Name | Red | Green | Blue | Saturation | Lightness | Hue angle | Wavelength |
|---|---|---|---|---|---|---|---|
| Orange | 87.06% | 49.41% | 29.02% | 69 | 58 | 21° | 591.08 nm |
| Sweet Pink | 98.04% | 80 % | 83.92% | 82% | 89% | 347° | 495.87 nm |
| Orchid  Pink | 89.8% | 74.21% | 70.98% | 48% | 80% | 5° | 595.2 nm |
| Adobe | 71.76% | 37.65% | 2.55% | 41% | 52% | 10° | 600.93 nm |
| Brown Dark | 34.51% | 25.01% | 17.25% | 28% | 24% | 35° | 611.37 nm |



Figure (7) Shows **a.** the brush stroke values (X & Y), **b.** a model stereotype and magnify the point of a part bearing the texture brush and shows wavelengths texture brush in the spectral space

## 4. Discussion

Brushstroke analysis was employed to identify the patterns statistically and define the optical properties of the brush strokes of the artist. It could be used during restoration (cleaning) to study changes in brush stork and help understand the technical style of the artist because it gives color charts indicating the distribution. Each color's tone, name, and number in the brush area is assigned a value in the internationally recognized color index by "ASTM" [50]. The computer numerical analysis of oil paintings to extract the texture of the brush is the fastest and best way in the analysis and compilation of data. In addition to the other examinations and analyses, e.g. FTIR, EDX-SEM, and XRD, the analysis of the brush texture is employed in painting documentation [51]. Brushstroke analysis using ENVI 5 passes through various stages. First, it is examined visually to identify the artistic style of the painter by taking and enlarging the distinctive part of the brush texture, which is called sgraffito [52]. Then, the quantitative measurement of

the percentage of each color illustrated that sweet pink was ranked first (96. 04%), saturation was (83.2%) and the wavelengths of orange-red was 495.85 nm [53]. The areas colored light orange were rated (87.06%), those colored adope (brown) were rated (71.76%), those colored dark brown were rated (30.59%) [54], and orchid pink was rated (89.8%). As for the properties, the brush was flat with rough hard hair, parallel lines, and perpendicular angles [55], fig. (8-a,b,c). SEM-EDX analysis of all samples pointed out that they contained silica, iron, and minerals' clay. Moreover, iron oxides are responsible for ochre color, including hematite ($Fe_2O_3$) and goethite (FeO(OH) suggesting that iron was the main chromophore for both red and yellow samples, respectively. However [56] other elements (Fe, Mg, Al, Si Ca, O, C, Na, and K) defined the colored oxide and helped ascertain provenance, such as quartz ($SiO_2$), feldspars (Na, K) $AlSi_3O_8$), and micas [57]. The counts of K and Fe observed in green sample indicated the concomitant use of malachite and celadonite (K(Al, FeIII), (FeII, Mg)] ($AlSi_3,Si_4$) $O_{10}$ ($OH_2$), showing that the green earth pigments were also used. The amounts of (Fe) and (pb) oxides in the yellow sample turned black or brown $Pb^{2+}$ were "seconddary" driers and active during polymerization [58]. Although the concentration of the lead paint (2.85%) could be much smaller and still be effective, an explanation for the Pb-bearing phase within the paint was best described by cation migration during the drying process, hypothetically by minor amounts of hydrolyzing oil, and migrated via diffusion into the paint layer [59]. The presence of clay in this layer might trap the migrating lead compound to form a spectrally distinct association, as evidence by the presence of (Si, Al, Mg, Ca). All earth pigments contributed to the development of bad paint films, such as (Si, Al, Mg, Ca, Na, k) oxide could actually have detrimental effects, causing brittleness and even delaminating the paint layers. Supplying the "active" metal ions, the film formation in drying oils was poor [60]. The earth pigments, that were exposed to degradation by a source of moisture, caused the movement of alkaline substances from the inner parts to the surface. Then, they were completely lost or reacted with the gasses of the air pollution into carbonates and sulfate. This interpreted the layers of white degradation on the surface. Calcium was rated 4.98% in the red samples, 5.28% in the yellow sample, and 0.85% in the sample, suggesting that calcite was used as a gesso layer or accompanied with earth colored. Thus, it was a result of the degradation processes due to the movement of calcium from the ground or earth colored to be deposited on the surface and reacted with air pollutants to form calcium carbonates and sulfate. XRD examination revealed the existence of gypsum. It is one of the most dangerous degradations because it, as a hygroscopic layer, absorbs and keeps water vapor. Consequently, water is always on the painting surface. A net of micro cracks on the surface, degradation, and weak and fragile colors of tracing lines with cracks were observed.
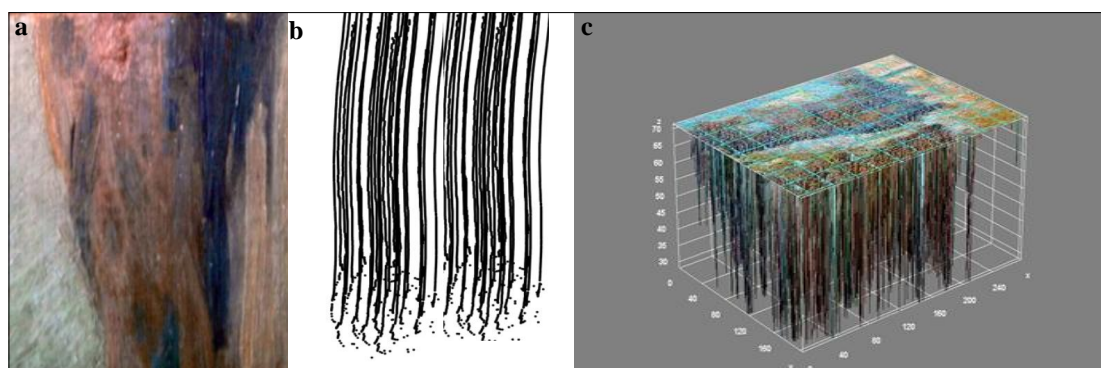


Figure (8) Shows **a.** a-brush lines, **b.** end edge Brushparallel, **c.**brush numerical value

## 5. Conclusion

*The work presented is focused on documentation a brushstroke visible as distinct marks on a surface by using ENVI 5 program which analyzed The brush texture to get information Quantitative and qualitative analysis such as, spectral, and spatial information about the texture of the brush., obtaining the spatial coordinates of brushstrokes, the wavelength of each color in brushstroke which is a distinctive color mark and the end of it's the brushstroke is either hard or soft stroke. This method is generalized to all archaeological drawings with colored texture. Furthermore, the brush texture analysis used during restoration to study changes to the brushstroke area.*

## References

[1] Frei, W. & Chen, C., (1977). Fast boundary detection: A generalization and a new algorithm, *IEEE Transactions on Computers,* Vol. 26 (10), pp: 988-998.

[2] Daviad, J. & James, R., (1995). Pyramid-based texture analysis/ synthesis, In: Susan, G. & Robert C. (eds.) *the 22nd Annual Conf. on Computer Graphics and Interactive Techniques*, Springer-Verlag, New York, pp: 229-238.

[3] Lukac, R., (2008). *Single-sensor imaging: methods and applications for digital cameras*, CRC press, USA.

[4] Zhao, H., Jin, X., Shen, J., Mao, X., & Feng, J., (2008). Real-time feature-aware video abstraction, *The Visual Computer,* Vol .24 (7-9), pp: 727-734.

[5] Maini, R. & Sohal, J., (2006). Performance evaluation of Prewitt edge detector for noisy images, *J. of Graphics, Vision and Image Processing,* Vol. 6 (3), pp: 39-46.

[6] Zhang, E., Mischaikow, K., Turk, G., & Turk, G., (2006). Vector field design on surfaces, *ACM Transactions on Graphics,* Vol. 25 (4), pp: 1294-1326.

[7] Hertzmann, A., (1998). Painterly rendering with curved brush strokes of multiple sizes, in: Cunningham, S., Bransford, W. & Cohen, M. (eds.) *25th Annual Conf. on Computer Graphics and Interactive Techniques*, ACM, NY, pp: 453-460.

[8] Haeberli, P., (1990). Paint by numbers: Abstract image representations, in: Baskett, F. (ed.) *Proceedings of the 17th Annual Conf. on Computer Graphics and Interactive Techniques*, ACM, Dallas, NY, Vol. 24 (4), pp: 207-214.

[9] Caelli, T. & Reye, D., (1993). On the classification of image regions by color, texture and shape, *Pattern Recognition,* Vol. 26 (4), pp: 461-470.

[10] Wang, S., Cai, K., Lu, J., Liu, X. & Wu, E., (2010). Real-time coherent stylization for augmented reality, *The Visual Computer*, vol. 26 (6-8), pp: 445-455.

[11] Chang, S., Yu, B. & Vetterli, M., (2000). Spatially adaptive wavelet thresholding with context modeling for image denoising, *IEEE Transactions on Image Processing*, Vol. 9 (90), pp: 1522-1531.

[12] Ciocca. G & Schettini, R., (1999). A relevance feedback mechanism for content-based image retrieval, *Information Processing & Management*, Vol. 35 (5), pp: 605-632

[13] Francus, P. & Karabanov, E., (2000). A computer-assisted thin-section study of Lake Baikal sediments: A tool for understanding sedimentary processes and deciphering their climatic signal, *Int. J. of Earth Sciences,* Vol. 89 (2), pp: 260-267.

[14] Raman, M. & Aggarwal, H., (2009). Study and comparison of various image edge detection techniques, *Int. J. of Image Processing*, Vol. 3 (1), pp: 1-12.

[15] Hong, L., Wan, Y. & Jain, A. (1998). Fingerprint image enhancement, *IEEE Transactions on Pattern Analysis and Machine Intelligence,* Vol. 20 (8), pp: 777-789.

[16] Lucchese, L. & Mitra, S., (2000). Filtering color images in the xyY color space, in: Zuliani, M., Bertelli, L., Kenney, C. & Manjunath, B. (eds.) *IEEE Int. Conf. on Image Processing*, *IEEE*, Vancouver, Vol . 3, pp: 500-533.

[17] Trahanias, P., Karakos, D. & Venetsanopoulos, A., (1996). Directional processing of color images: Theory and experimental results, *IEEE Transactions on Image Processing,* Vol. 5 (6), pp: 868-880.

[18] Langfelder, G., Zaraga, F. & Longoni, A., (2009). Tunable spectral responses in a color-sensitive CMOS pixel for imaging applications, *IEEE Transactions on Electron Devices,* Vol. 56 (11), pp: 965-875.

[19] Hough, H., (1991). *Satellite Surveillance*, Breakout Productions Inc, USA.

[20] Ritter, L., Li, W., Curless, B., Agrawala, M. & Salesin, D., (2006). Painting with texture, in: Akenine-Möller, T. & Heidrich, W. (eds.) *Proceedings 17th Eurographics Conf. on Rendering Techniques,* Eurographics Association, Italy, pp: 371-376.

[21] Kolar, J., Strlic, M., Pentzien, S. & Kautek, W., (2000). Near-UV, visible and IR pulsed laser light interaction with cellulose, *Applied Physics A,* Vol. 71 (1), pp: 87-90.

[22] Thevenet, L., Dupont, D. & Caze, C., (2002). A comprehensive physical model for light reflection in textiles for computer graphics applications, *AUTEX Research Journal*, Vol. 2, pp: 190-198.

[23] Combettes, P. & Pesquet, J., (2010). Image restoration subject to a total variation constraint, *IEEE Transactions on Image Processing*, Vol. 13 (9), PP: 1213-1222.

[24] Aschwanden, M., (2010). Image processing techniques and feature recognition in solar physics, *Solar Physics*, Vol. 262 (2), pp: 235-275.

[25] Sebastian, P., Voon, Y. V. & Comley, R., (2008). The effect of colour space on tracking robustness, in: Luo, F., Zigong, M. (eds.) *Proceedings 3rd IEEE Conf. on Industrial Electronics and Applications,* IEEE, Singapore, pp: 2512-2516.

[26] Krinsley, D. & Doornkamp, J. (2011). *Atlas of quartz sand surface textures*, Cambridge University Press, UK.

[27] Goldstein, J., Newbury, D., Joy, D. C., Lyman, C., Echlin, P., Lifshin, E. & Michael, J. R., (2003). *Scanning Electron Microscopy and X-Ray Microanalysis*, Springer, NY.

[28] Drits, V., Środoń, J., & Eberl, D. D., (1997). XRD measurement of mean crystallite thickness of illite and illite/smectite: Reappraisal of the Kubler index and the Scherrer equation, *Clays and Clay Minerals*, Vol. 45 (3), pp: 461-475.

[29] Mantler, M., & Schreiner, M., (2001). X-ray analysis of objects of art and archaeology, *J. of Radio Analytical and Nuclear Chemistry*, Vol. 247 (3), pp: 635-644.

[30] Meilunas, R., Bentsen, J. & Steinberg, A., (1990). Analysis of aged paint binders by FTIR spectroscopy, *Studies in Conservation,* Vol. 35 (1), pp: 3-22.

[31] Teo, T., (2011). Bias compensation in a rigorous sensor model and rational function model for high-resolution satellite images, *Photogrammetric Engineering and Remote Sensing,* Vol .77(12), pp: 1211-1220.

[32] Eastaugh, N., Walsh, V., Chaplin, T. & Siddall, R., (2008). *Pigment compendium: A dictionary and optical microscopy of historic pigments*, Butterworth- Heinemann, London.

[33] Shimadzu, Y. & Van Den Berg, K., (2006). On metal soap related colour and transparency changes in a 19th C painting by Millais, in: Boon, J. & Ferreira, E. (eds.) *Reporting Highlights of the De Mayerne Programme,* the Hauge: Netherlands Org. for Scientific Research (NWO), Netherlands pp: 43-52.

[34] Hertzmann, A. (2003). A survey of stroke-based rendering, IEEE *Computer Graphics and Applications,* (4), pp: 70-81.

[35] Perona, P. & Malik, J., (1990). Scale-space and edge detection using anisotropic diffusion, *IEEE Transactions on Pattern Analysis and Machine Intelligence*, Vol. 12 (7), pp: 629-639.

[36] Woodham, R., (1981). Analysing images of curved surfaces, *Artificial Intelligence*, Vol. 17 (1-3), pp: 117- 140.

[37] Lukáč, M., Fišer, J., Asente, P., Lu, J., Shechtman, E. & D. Sýkora (2015). Brushables: Example-based edge-aware directional texture painting in: Mitra, N., Stam, J. & Xu, K. (eds.) *Proceedings Computer Graphics Forum*, Wiley & Sons Ltd, UK, Vol. 34 (7), pp: 257-267.

[38] Zheng, M., Yan, Z., Zhibin Z. & hengxing, S., (2014). Image Palette: brushstroke synthesis-based style transfer, in: Keyser, J., Kim, Y. & Wonka, P. (eds.) *Pacific Graphics*, The Eurographics Association, Vol. 76 (6), pp: 7989-8010.

[39] Terrance Booth, D., Cox, S., Fifield, C., Phillips, M. & Williamson, N., (2005). Image analysis compared with other methods for measuring ground cover, *Arid Land Research and Management*, Vol .19 (2), pp: 91-100.

[40] Lukáč, M., Fišer, J., Bazin, J., Jamriška, O., Sorkine-Hornung, A., & Sýkora, D., (2013). Painting by feature: texture boundaries for example-based image creation, *J. ACM Transactions on Graphics*, Vol. 32 (4), p. 116.

[41] Anderse, C., Bonaduce, I., Andreotti, A., van Lanschot, J. & Vila, A., (2017). Characterisation of preparation layers in nine Danish Golden Age canvas paintings by SEM-EDX, FTIR and GC-MS, *Heritage Science*, Vol. 5 (1), p.34.

[42] Sawin, M., (1995). *Surrealism in exile and the beginning of the New York school*, MIT Press, USA.

[43] Papadakis, M., Orphanos, Y., Kogou, S., Melessanaki, K., Pouli, P. & Fotakis, C. (2011). IRIS: a novel spectral imaging system for the analysis of cultural heritage objects, in: Pezzati, L. & Salimbeni, R. (eds.), O3A: Optics for arts, architecture, and archaeology III, International Society For Optics and Photonics, Munich, Germany, Vol. 8084, pp: 1-6

[44] Salvadó, N., Pradell, T., Pantos, E., Papiz, M., Molera, J., Seco, M. & Vendrell-Saz, M., (2002). Identification of copper-based green pigments in Jaume Huguet's Gothic altarpieces by Fourier transform infrared micro spectroscopy and synchrotron radiation X-ray diffraction, *J. of Synchrotron Radiation,* Vol .9 (4), pp: 215-222.

[45] Bottcher, M., Gehlken, P. & Steele, D., (1997). Characterization of inorganic and biogenic Magnesian calcites by Fourier Transform infrared spectroscopy, *Solid State Ionic*, Vol. 101, pp: 1379-1385.

[46] Bonaduce, I., Andreotti. A., (2009). *Organic mass spectrometry in art and archaeology*, John Wiley & Sons, UK.

[47] Gorman, O', L., & Kasturi , R., (1995). *Document image analysis*, IEEE Computer Society Press Los Alamitos, California.

[48] Pabby, A., Rizvi, S. & Requena, A. M., (2008). *Handbook of membrane separations: Chemical, pharmacyeutical, food, and biotechnological applications*, CRC press, NY.

[49] Kasturi, R., O'gorman, L. & Govindaraju, V., (2002). Document image analysis: A primer, *Sādhanā*, Vol. 27 (1), pp: 3-22.

[50] Majnarić, I., Mirković, I., Birta, A. & Mustač, S., (2013). The influence of the extreme thick applied layers of varnish on color properties of led UV curing inkjet prints, in: MacDonald, L., Westland, S. Wuerger, S. (eds.) *12th Congress of AIC Colour Conf. Proceedings,* Wiley Pub. Scientific, Newcastle Upon, pp: 234-235.

[51] Liu, H., Huang, M., Cui, G., Ronnier Luo, M. & Melgosa, M., (2013). Color-difference evaluation for digital

images using a categorical judgment method, *J. of the Optical Society of America A*, Vol. 30(4), pp: 616-626

[52] Plata, C., Nieves, J., Valero, E. & Romero, J., (2009). Trichromatic red-green-blue camera used for the recovery of albedo and reflectance of rough-textured surfaces under different illumination conditions, *Applied Optics*, Vol. 48 (19), pp: 3643-3653.

[53] Tony, C., & Shen, J., (2005). *Image processing and analysis: Variation PDE wavelet and stochastic methods*, 1st ed., Society for Industrial and Applied Mathematics, USA.

[54] Shin, M., Goldgof, D. & Bowyer, K., (2001). Comparison of edge detector performance through use in an object recognition task, *Computer Vision and Image Understanding*, Vol .84 (1), pp: 160-178.

[55], Roy S, Krueger, J. & Swicklik, M., (2002). Multiple pigment selection for in painting using visible reflectance spectrophotometry, *Studies in Conservation*, Vol. 47(1), pp: 46-61.

[56] Bansal, B., Saini, J., Bansal, V. & Kaur, G., (2012). Comparison of various edge detection techniques, *J. of Information and Operations Management*, Vol. 3 (1), pp: 103- 106.

[57] Saunders, D. & Kirby, L., (2004). The effect of relative humidity on artists' pigments, *National Gallery Technical Bulletin,* Vol. 25, pp: 62-72.

[58] Estaugh, N., Walsh, V., Chaplin, T. & Siddall, R., (2004). *The pigment compendium: Optical microscopy of historical pigments,* Elsevier, Oxford.

[59] Hradil, D. & Hradilová, J., (2012). Microanalysis of pigments in painted artworks, *Archaeometry and Cultural Heritage,* pp: 79-90.

[60] Tumosa, C. & Mecklenburg, M., (2005). The influence of lead ions on the drying of oils, *Studies in Conservation,* Vol .50 (1), pp: 39-47.